ISSN 0021-3640, JETP Letters, 2023, Vol. 118, No. 5, pp. 321–327. © The Author(s), 2023. This article is an open access publication.
Russian Text © The Author(s), 2023, published in Pis'ma v Zhurnal Eksperimental'noi i Teoreticheskoi Fiziki, 2023, Vol. 118, No. 5, pp. 323–329.

CONDENSED MATTER

Magnetic Structure and the Spin-Crossover Mechanism in Ludwigite Co_3BO_5

N. G. Zamkova[a,*], V. S. Zhandun[a], and S. G. Ovchinnikov[a,b]

[a] *Kirensky Institute of Physics, Federal Research Center KSC, Siberian Branch, Russian Academy of Sciences, Krasnoyarsk, 660036 Russia*

[b] *Siberian Federal University, Krasnoyarsk, 660041 Russia*

**e-mail: ngzamkova@gmail.com*

Received July 19, 2023; revised July 19, 2023; accepted July 25, 2023

A spin-crossover mechanism in ludwigite Co_3BO_5 is proposed on the basis of the DFT calculation with SCAN potentials. The role of separate exchange interactions in the establishment of the long-range magnetic order is demonstrated within the Monte Carlo method.

DOI: 10.1134/S0021364023602555

1. INTRODUCTION

Oxyborates with the ludwigite structure and the general formula $M^{2+}M^{3+}O_2BO_3$ have a wide variety of electronic and magnetic properties depending on the composition. A number of interesting features can be found in compounds with the ludwigite structure: low-dimensional magnetic systems (triads and layers), coexistence of several magnetic sublattices, coexistence of paramagnetism and magnetic order, various combinations of transition metals with mixed valence in the chemical composition, and their nonrandom distribution over different crystallographic sites. The ludwigite structure can include various M^{2+} and M^{3+} elements, but only two homometallic ludwigites Fe_3BO_5 and Co_3BO_5 with transition metal atoms are experimentally known to date [1–5]. Despite similar crystal structures, the two compounds have very different physical properties. In particular, Fe_3BO_5 undergoes a structural transition with the doubling of the lattice parameter c at room temperature, and then two magnetic transitions at $T_{N1} = 112$ K and $T_{N2} = 70$ K, corresponding to the independent ordering of different magnetic sublattices [1, 2]. On the contrary, Co_3BO_5 is structurally stable and undergoes a magnetic transition at a temperature of $\sim$42 K [3, 4]. It is assumed in [2] that the structural transition in Fe_3BO_5 is due to the dimerization of iron cations in one of the triads and the formation of charge density waves. The situation differs in ludwigite Co_3BO_5: to avoid structural distortions, the Co^{3+} ion transfers to the low-spin state. Thus, one of the main differences between ludwigites Fe_3BO_5 and Co_3BO_5 is the spin crossover in Co_3BO_5 [3, 4]. Both compounds were studied in detail experimentally and theoretically, in particular, in ab initio calculations [5–8]. However, main attention in calculations is paid to the magnetic structure of these ludwigites, while the spin-crossover mechanism in Co_3BO_5 remains unclear. The purpose of this work is an ab initio study of exchange interactions and the spin-crossover mechanism in Co_3BO_5. The spin crossover is usually described as the intersection of terms of two localized spins, but here we show the crossover mechanism in band terms.

2. CALCULATION DETAILS

The calculations were carried out in the Vienna Ab initio Simulation Package (VASP) [9, 10] using PAW–PBE pseudopotentials [11, 12]. The configuration of valence electrons for Co, B, and O ions was taken as $3d^74s^2$, $2s^22p^1$, and $2s^22p^4$, respectively. The exchange-correlation functional was taken into account in the generalized gradient approximation (GGA). The number of plane waves was limited by an energy of 520 eV. A $4 \times 2 \times 11$ Monkhorst–Pack grid was used to optimize crystal structures [13]. The parameters and coordinates of the atoms were optimized until the residual force on each ion became less than 1 meV/A. The group-theoretical analysis of magnetic structures was performed in the FullProf (BASIREPS) package [14] for wave vectors $\mathbf{k} = (0,0,0)$ and $\mathbf{k} = (0,0,0.5)$. The GGA + U calculations were performed in the Dudarev scheme [15].

3. MAGNETIC STRUCTURE

The ludwigite structure with the space group *Pbam* (no. 55) is conventionally presented in the form of a ladder structure. In the ludwigite structure, transition

metal atoms occupy four nonequivalent $2a$, $2d$, $4g$, and $4h$ sites. Atoms at the $2a$ and $4g$ sites form a three-step ladder or triad 3–1–3, and atoms at the $2d$ and $4h$ sites form the second triad 4–2–4 (Fig. 1). In ludwigite Co_3BO_5, the triad 3–1–3 is occupied by Co^{2+} ions, and the triad 4–2–4 is occupied by Co^{2+} ions at the $2d$ sites, and Co^{3+} ions at the $4h$ sites. All cobalt atoms are located in highly distorted oxygen octahedra.

As shown in [3, 4], Co_3BO_5 undergoes a magnetic transition to a completely ordered state at $T_N = 42$ K, while trivalent cobalt ions at the $4h$ sites are in the (LS) low-spin state. At high temperatures $T > 500$ K, these ions transfer to a high-spin (HS) state. The magnetic structure (Fig. 1) of ludwigite Co_3BO_5 is determined in [3, 4]. The experimental magnetic structure is collinear and, according to the group-theoretical analysis carried out in [3, 5], is described by one irreducible representation for all magnetic sublattices $\tau5(y)$ with the eigenvector

$$\begin{array}{cccccc} & 2a & 2d & 4g & 4h \\ \text{LS} & -- & ++ & ++++ & 0000 \\ \text{HS} & -- & ++ & ++++ & ---- \end{array}.$$

To determine the magnetic ground state in ludwigite Co_3BO_5, we calculated the total energies of a number of collinear and noncollinear magnetic configurations, which were constructed according to the irreducible representation of the space group *Pbam* at $k = 0$ and $k = (0,0,0.5)$ the space group *Pbnm* at $k = 0$ (see Table 1). In particular, the magnetic configurations for compounds with the ludwigite structure were considered in [1, 3–7, 16]. The total energies for all magnetic configurations were calculated in the GGA + U approximation with $U = 4$ eV for the cobalt atom. The magnetic configuration found in the experiment [3, 4], but with the Co^{3+} ion at the $4g$ site in the HS state (Fig. 1), was most energetically favorable at this parameter U.

In both triads 3–1–3 and 4–2–4, the ordering of atoms is antiferromagnetic, while the ordering of triads along the c axis is ferromagnetic. However, it is impossible to unambiguously determine the energy benefit of HS or LS configurations in the GGA + U approximation, which largely depends on the parameter U.

To avoid such ambiguity in determining the ground state, the total energy of a given magnetic configuration with the Co^{3+} ion in the HS and LS states was calculated in a more rigorous approximation with SCAN potentials [17]. When calculating energies, complete relaxation of the structure was carried out in terms of lattice parameters and atomic coordinates. The calculation results together with experimental data are given in Table 2. As seen, the SCAN calculation indicates that the magnetic configuration with the Co^{3+} ion in the LS state is most energetically favorable at low temperatures.

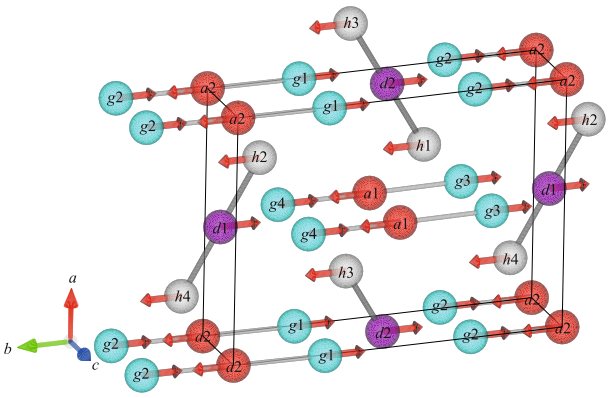

Fig. 1. (Color online) Magnetic structure of ludwigite Co_3BO_5. Only cobalt atoms are shown.

According to [4], the transition of Co^{3+} ions to the HS state at a high temperature $T > 500$ K is accompanied by an increase in the unit cell volume by 5%. However, in our calculation, the unit cell volume after the complete optimization of the structure with the Co^{3+} ion in the HS state hardly changed because the high-temperature phase is not an equilibrium structure at zero temperature. Therefore, to simulate the thermal expansion of the lattice in the high-temperature phase, a unit cell obtained by applying a hydrostatic pressure of $P = -10$ GPa was used in the calculation of the total energies for the HS and LS states of Co^{3+}. In this case, the unit cell volume increases by 5.7% compared to the unit cell volume in the ground LS state. As seen in Table 2 (the last two columns), the transition of the Co^{3+} ion to the HS state becomes

Table 1. Decomposition of the magnetic representation of the space group *Pbam* in irreducible representations at $k = 0$ and $k = (0,0,0.5)$ the space group *Pbnm* at $k = 0$

	Pbam, $k = 0$
$2a$, $2d$	$\tau1 + \tau3 + 2\tau5 + 2\tau7$
$4g$, $4h$	$\tau1 + 2\tau2 + \tau3 + 2\tau4 + 2\tau5 + \tau6 + 2\tau7 + \tau8$
	Pbam, $k = (0,0,0.5)$
$2a$	$\tau1 + \tau3 + 2\tau5 + 2\tau7$
$2d$	$\tau2 + tau4 + 2\tau6 + 2\tau8$
$4g$	$\tau1 + 2\tau2 + \tau3 + 2\tau4 + 2\tau5 + \tau6 + 2\tau7 + \tau8$
$4h$	$2\tau1 + \tau2 + 2\tau3 + \tau4 + \tau5 + 2\tau6 + \tau7 + 2\tau8$
	Pbnm $k = 0$
$4a$	$3\tau1 + 3\tau3 + 3\tau5 + 3\tau7$
$4c$	$\tau1 + 2\tau2 + 2\tau3 + \tau4 + \tau5 + 2\tau6 + 2\tau7 + \tau8$
$8d$	$3\tau1 + 3\tau2 + 3\tau3 + 3\tau4 + 3\tau5 + 3\tau6 + 37tau7 + 3\tau8$

Table 2. Experimental and calculated lattice parameters a, b, and c using SCAN potentials, unit cell volume V, and magnetic moments of cobalt ions at the 2a (M1), 2d (M2), 4g (M3), and 4h (M4) sites in high- and low-spin configurations. The last two lines give the energies of the low-spin state with respect to the high-spin state and the energy gap

			SCAN			
	Experiment [3, 4]		Low-temperature phase		High-temperature phase	
	HS (700 K)	LS (2 K)	HS	LS	HS	LS
a, Å	9.27	9.32	9.16	9.28	9.26	
b, Å	12.25	11.95	12.14	11.88	12.26	
c, Å	3.05	2.96	3.00	2.95	3.12	
V, Å^3	346.35	329.67	334.26	337.52	357.94	
M1, μ_B		3.4	2.46	2.62	2.56	2.62
M2, μ_B		−3.06	−2.68	−2.60	−2.68	−2.65
M3, μ_B		−3.38	−2.85	−2.63	−2.9	−2.71
M4, μ_B		0.11	2.32	−0.07	2.38	0.15
E, eV			0.0	−2.1973	0.0	0.4421
E_g, eV		1.7	0.0	0.4	0.0	0.0

energetically favorable at such an increase in the volume, which is consistent with experiment [3, 4].

4. SPIN CROSSOVER

Figure 2 shows d electron densities of HS and LS states at the 4h site in the Co^{3+} ion. It is well known that the spin state of $d6$ transition metal ions in an octahedral environment is determined by the competition between the intra-atomic exchange and the crystal field energy. The exchange energy favors the HS state with the configuration $(t_{2g}^4 e_g^2)$, while the crystal field favors the LS state $(t_{2g}^6 e_g^0)$. However, the d electron density of states in the Co^{3+} ion has no pronounced peaks, which could be interpreted as the splitting of d levels in the octahedral crystal field (Fig. 2), because the oxygen octahedra in the ludwigite structure are distorted, and, as a result, the cobalt atoms are in a crystal field of lower symmetry (triclinic) and the mechanism for the transition from the LS to HS state is more complicated. The d electrons in the Co^{3+} ion form the energy bands ~4–6 eV wide, and the density of states contains well-defined peaks near the Fermi energy. During the transition from the LS to HS state, the splitting between spin-up and spin-down states of t_{2g} and e_g electrons increases. In the HS state, the peaks corresponding to spin-up electrons with spin up are shifted below the Fermi energy, and these states become occupied. At the same time, the peaks corresponding to spin-down electrons are shifted to higher energies and begin to be depleted.

In both HS and LS configurations, the t_{2g} and e_g states forming pronounced peaks in the density of states have the same energies. Nevertheless, different d orbitals make different contributions to the magnetic moment of the Co^{3+} ion in the HS state. The formation mechanism of the magnetic moment is the same for all types of d orbitals and is associated with the splitting between spin-up and spin-down electron states (Table 3, the first two columns), but this splitting differs for d electrons of different symmetries. The occupation numbers of energy bands for d electrons of different symmetries are presented in the last column of Table 3. The largest contribution to the magnetic moment during the transition of the cobalt atom to the HS state comes from the d_{xy}, d_{xz}, and d_z^2 orbitals.

5. MONTE CARLO SIMULATION OF THE MAGNETIC TRANSITION

The structural elements in the ludwigite structure are usually distinguished in the form of three-step ladders or triads 3–1–3 and 4–2–4. In particular, two magnetic transitions associated with the successive ordering of such triads are observed in ludwigite Fe_3BO_5. Unlike Fe_3BO_5, the 4h site in cobalt ludwigite is occupied by the Co^{3+} ion, which is in the low-spin state below room temperature, and the triad 4–2–4 is destroyed. Figure 3 shows the main exchange interactions in ludwigite Co_3BO_5 with the Co^{3+} ion in the LS state. Exchange interactions were calculated within the Ising model according to the algorithm described in [18]. In this case, the magnetic moment of divalent cobalt ions at the 2a, 2d, and 4g sites was set equal to a calculated value of $\approx 2.65\mu_B$, and the magnetic moment of the trivalent cobalt ion was zero. The determined exchange interactions are given in Table 4.

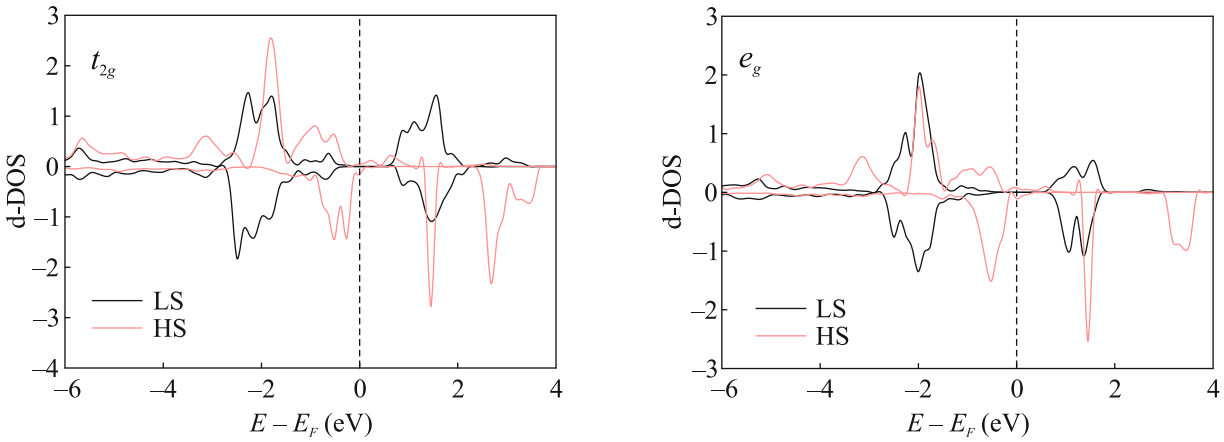

Fig. 2. (Color online) Density of states of t_{2g} and e_g electrons in ludwigite Co_3BO_5 in the (light brown line) high- and (black line) low-spin states.

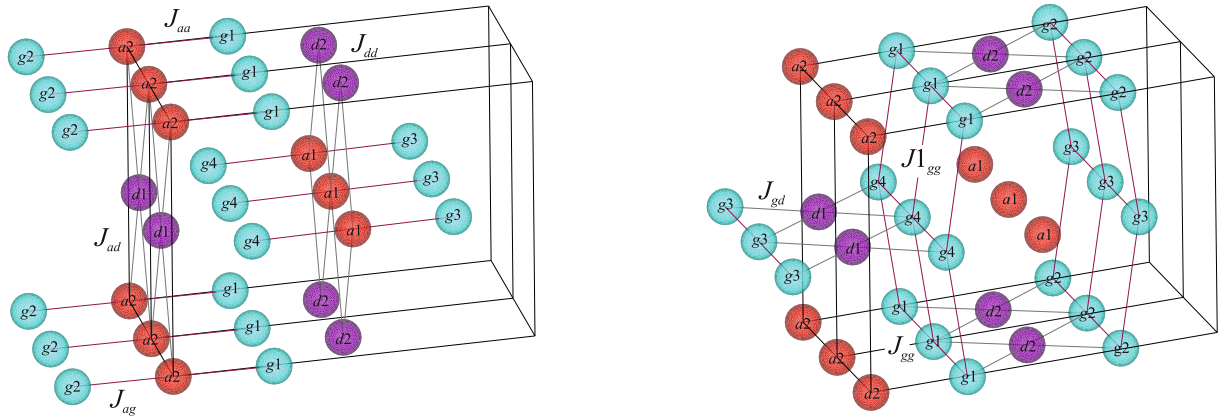

Fig. 3. Exchange interactions in ludwigite Co_3BO_5 in the low-spin configuration. Only magnetic cobalt ions at the 2*a*, 2*d*, and 4*g* sites are shown.

Here, the strongest interactions are ferromagnetic interactions between Co^{2+} ions at the 2*a* (J_{aa}) and 2*d* (J_{dd}) sites along the *c* axis, and antiferromagnetic interactions between Co^{2+} ions at 2*a* and 4*g* sites (J_{ag}) in the triads 3–1–3 and at the 2*a* and 2*d* (J_{ad}) sites in *ac* planes. These interactions allow one to distinguish two structural units in ludwigite Co_3BO_5: the triads 3–1–3, containing ions at the 2*a* and 4*g* sites, and *ac* planes formed by ions at the 2*a* and 2*d* sites. Triads are coupled by ferromagnetic interactions between ions at 4*g* sites along the *c* axis (J_{gg}) and along the *a* axis ($J1_{gg}$), and weak antiferromagnetic interactions in the *bc* plane (J_{dg}).

Using the found exchange constants, the Monte Carlo method was used to calculate the magnetic transition temperature in Co_3BO_5 with the Co^{3+} ion in the LS state. Figure 4 shows the temperature dependences of (a) the magnetization of individual magnetic sublattices and total magnetization and (b) the magnetic susceptibility. All sublattices are ordered at the same temperature $T_c \approx 118$ K.

The magnetic transition temperature obtained by the Monte Carlo method is approximately three times higher than the experimental value $T_c \approx 42$ K [3, 4]; this difference is typical of Monte Carlo calculations. Nevertheless, Monte Carlo simulations allow the analysis of the role of individual exchange interactions in the ordering of the magnetic moments of cobalt ions. The important role of the interaction of the triads 3–1–3 via the cobalt ion at the 2*d* site in the establishment of the long-range magnetic order was noted in [3]. In fact, the triads 3–1–3 are coupled by the strong ferromagnetic interaction J_{ad} and weak antiferromagnetic interaction J_{dg} via the ion at the 2*d* site. We

Table 3. (First column) Density of states of *d* electrons of different symmetries and (second column) the scheme of levels for spin-up and spin-down electrons in the (light brown line) high- and (black line) low-spin states. The last column shows the occupation numbers of the corresponding energy bands

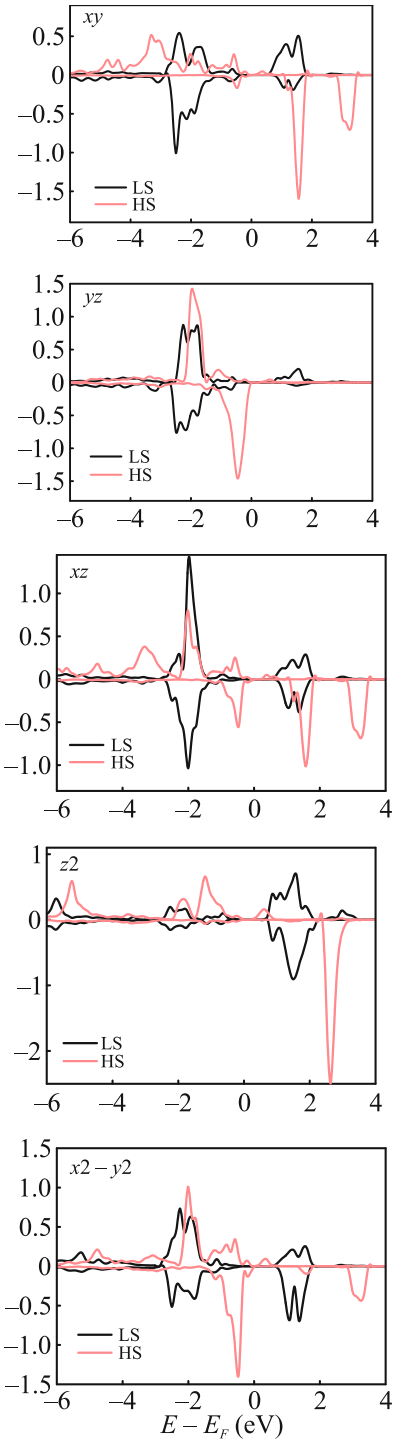	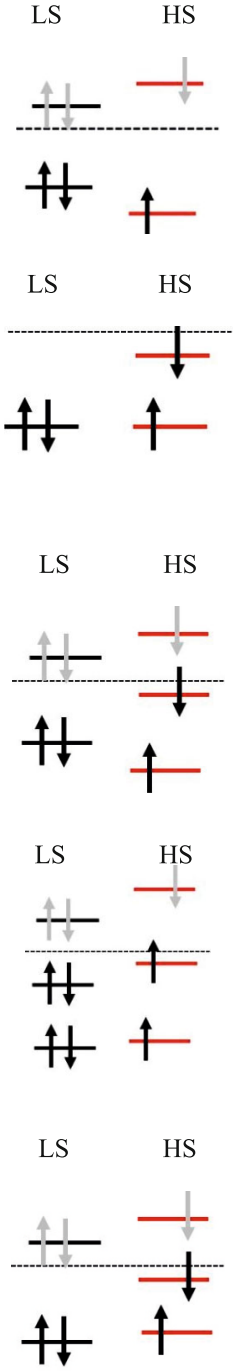	LS HS $n_\uparrow = 0.55$ $n_\uparrow = 0.88$ $n_\downarrow = 0.81$ $n_\downarrow = 0.11$ $S^z = -0.26$ $S^z = 0.77$ LS HS $n_\uparrow = 0.77$ $n_\uparrow = 0.86$ $n_\downarrow = 0.87$ $n_\downarrow = 0.86$ $S^z = -0.1$ $S^z = 0.0$ LS HS $n_\uparrow = 0.39$ $n_\uparrow = 0.85$ $n_\downarrow = 0.32$ $n_\downarrow = 0.14$ $S^z = 0.07$ $S^z = 0.71$ LS HS $n_\uparrow = 0.7$ $n_\uparrow = 0.88$ $n_\downarrow = 0.7$ $n_\downarrow = 0.23$ $S^z = 0.0$ $S^z = 0.65$ LS HS $n_\uparrow = 0.73$ $n_\uparrow = 0.88$ $n_\downarrow = 0.52$ $n_\downarrow = 0.66$ $S^z = 0.21$ $S^z = 0.22$

Table 4. Exchange interactions in ludwigite Co_3BO_5

J_{dd}	J_{aa}	J_{ag}	J_{ad}	J_{gg}	$J1_{gg}$	J_{dg}
59.9 K	55.1 K	−38.6 K	−19.6 K	8.5 K	8.2 K	−3.2 K

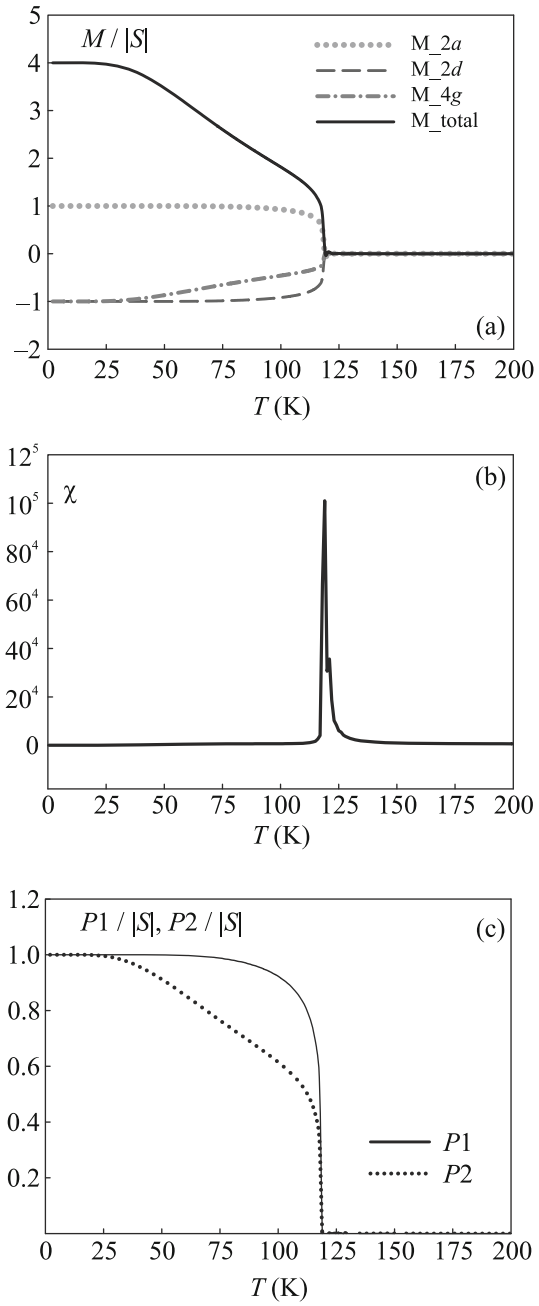

Fig. 4. Temperature dependences of (a) the total magnetization and magnetizations of individual magnetic sublattices, (b) the magnetic susceptibility, and (c) the order parameters $P1$ and $P2$ (see the main text) at $|S| = 2.65\mu_B$.

introduce two order parameters responsible for the ordering of magnetic moments in the *ac* plane:

$$P1 = \frac{1}{4}(S_{a1} - S_{d2} + S_{a2} - S_{d1}),$$

and in the triads 3–1–3:

$$P2 = \frac{1}{6}(S_{a1} - S_{g3} - S_{g4} + S_{a2} - S_{g1} - S_{g2}).$$

Temperature dependences of the order parameters $P1$ and $P2$ are shown in Fig. 4c. The disordering of triads starts at a temperature of ~50 K, but the long-range order is preserved up to higher temperatures because of the stronger in-plane interaction J_{ad}. Thus, the magnetic transition temperature is determined by interactions in the *ac* plane.

CONCLUSIONS

To summarize, the magnetic structure of the ludwigite Co_3BO_5B has been determined within the density functional theory calculation using the SCAN potential. It has been shown that the collinear antiferromagnetic structure with the Co^{3+} ion in the low-spin state is energetically favorable at low temperatures. The calculation of the electron structure of the Co^{3+} ion in low- and high-spin states has allowed us to propose a spin-crossover mechanism associated with the splitting between spin-up and spin-down electron states. The exchange interactions in Co_3BO_5 with the Co^{3+} ion in the low-spin state have been estimated within the Ising model. It has been shown that the magnetic transition temperature is determined by the magnetic interactions between ions located in the *ac* plane.

FUNDING

This work was supported by the Russian Science Foundation (no. 22-22-20024 https://rscf.ru/project/22-22-20024/) and the Krasnoyarsk Regional Science Foundation.

CONFLICT OF INTEREST

The authors declare that they have no conflicts of interest.

REFERENCES

1. P. Bordet and E. Suard, Phys. Rev. B **79**, 144408 (2009).

2. M. Mir, J. Janczakb, and Y. P. Mascarenhas, J. Appl. Crystallogr. **39**, 42 (2006).
3. D. C. Freitas, C. P. C. Medrano, D. R. Sanchez, M. Nunez Regueiro, J. A. Rodríguez-Velamazán, and M. A. Continentino, Phys. Rev. B **94**, 174409 (2016).
4. N. V. Kazak, M. S. Platunov, Yu. V. Knyazev, M. S. Molokeev, M. V. Gorev, S. G. Ovchinnikov, J. Bartolomé, A. Arauzo, V. V. Yumashev, S. Yu. Gavrilkin, F. Wilhelm, and A. Rogalev, Phys. Rev. B **103**, 094445 (2021).
5. Yu. V. Knyazev, N. V. Kazak, I. I. Nazarenko, S. N. Sofronova, N. D. Rostovtsev, J. Bartolomec, A. Arauzod, and S. G. Ovchinnikov, J. Magn. Magn. Mater. **474**, 493 (2019).
6. M. Matos, J. Terra, D. E. Ellis, and A. S. Pimentel, J. Magn. Magn. Mater. **374**, 148 (2015).
7. M. Matos, J. Terra, and D. E. Ellis, Phys. Status Solidi B **256**, 1900298 (2019).
8. E. Vallejo and M. Avignon, J. Magn. Magn. Mater. **435**, 33 (2017).
9. G. Kresse and J. Furthmuller, Phys. Rev. B **54**, 11169 (1996).
10. P. E. Blochl, Phys. Rev. B **50**, 17953 (1994).
11. G. Kresse and D. Joubert, Phys. Rev. B **59**, 1758 (1999).
12. P. Perdew, K. Burke, and M. Ernzerhof, Phys. Rev. Lett. **77**, 3865 (1996).
13. H. J. Monkhorst and J. D. Pack, Phys. Rev. B **13**, 5188 (1976).
14. J. Rodriguez-Carvajal, Phys. B (Amsterdam, Neth.) **192**, 55 (1993).
15. S. L. Dudarev, G. A. Botton, S. Y. Savrasov, C. J. Humphreys, and A. P. Sutton, Phys. Rev. B **57**, 1505 (1998).
16. F. Damay, J. Sottmann, F. Lainé, L. Chaix, M. Poienar, P. Beran, E. Elkaim, F. Fauth, L. Nataf, A. Guesdon, A. Maignan, and C. Martin, Phys. Rev. B **101**, 094418 (2020).
17. J. Sun, A. Ruzsinszky, and J. P. Perdew, Phys. Rev. Lett. **115**, 036402 (2015).
18. H. Xiang, Ch. Lee, H.-J. Koo, X. Gonga, and M.-H. Whangbo, Dalton Trans. **42**, 823 (2013).

Translated by L. Mosina